RESEARCH ARTICLE

MEDICAL PHYSICS

The dirty and clean dose concept: Towards creating proton therapy treatment plans with a photon-like dose response

Lena Heuchel[1] | **Christian Hahn[1,2,3]** | **Jakob Ödén[4]** | **Erik Traneus[4]** | **Jörg Wulff[5,6]** | **Beate Timmermann[5,6,7,8]** | **Christian Bäumer[1,5,6,8]** | **Armin Lühr[1]**

[1]Department of Physics, TU Dortmund University, Dortmund, Germany

[2]OncoRay-National Center of Radiation Research in Oncology, Faculty of Medicine and University Hospital Carl Gustav Carus, Technische Universität Dresden, Helmholtz-Zentrum Dresden-Rossendorf, Dresden, Germany

[3]Department of Radiotherapy and Radiation Oncology, Faculty of Medicine and University Hospital Carl Gustav Carus, Technische Universität Dresden, Dresden, Germany

[4]RaySearch Laboratories AB, Stockholm, Sweden

[5]West German Proton Therapy Center Essen, Essen, Germany

[6]West German Cancer Center (WTZ), University Hospital Essen, Essen, Germany

[7]Department of Particle Therapy, University Hospital Essen, Essen, Germany

[8]German Cancer Consortium (DKTK) and German Cancer Research Center (DKFZ), Essen, Germany

Correspondence
Lena Heuchel, Otto-Hahn-Str. 4, Dortmund 44227, Germany.
Email: Lena.Heuchel@tu-dortmund.de

Abstract

Background: Applying tolerance doses for organs at risk (OAR) from photon therapy introduces uncertainties in proton therapy when assuming a constant relative biological effectiveness (RBE) of 1.1.

Purpose: This work introduces the novel dirty and clean dose concept, which allows for creating treatment plans with a more photon-like dose response for OAR and, thus, less uncertainties when applying photon-based tolerance doses.

Methods: The concept divides the 1.1-weighted dose distribution into two parts: the clean and the dirty dose. The clean and dirty dose are deposited by protons with a linear energy transfer (LET) below and above a set LET threshold, respectively. For the former, a photon-like dose response is assumed, while for the latter, the RBE might exceed 1.1. To reduce the dirty dose in OAR, a MaxDirtyDose objective was added in treatment plan optimization. It requires setting two parameters: LET threshold and max dirty dose level. A simple geometry consisting of one target volume and one OAR in water was used to study the reduction in dirty dose in the OAR depending on the choice of the two MaxDirtyDose objective parameters during plan optimization. The best performing parameter combinations were used to create multiple dirty dose optimized (DDopt) treatment plans for two cranial patient cases. For each DDopt plan, 1.1-weighted dose, variable RBE-weighted dose using the Wedenberg RBE model and dose-average LET_d distributions as well as resulting normal tissue complication probability (NTCP) values were calculated and compared to the reference plan (RefPlan) without MaxDirtyDose objectives.

Results: In the water phantom studies, LET thresholds between 1.5 and 2.5 keV/μm yielded the best plans and were subsequently used. For the patient cases, nearly all DDopt plans led to a reduced Wedenberg dose in critical OAR. This reduction resulted from an LET reduction and translated into an NTCP reduction of up to 19 percentage points compared to the RefPlan. The 1.1-weighted dose in the OARs was slightly increased (patient 1: 0.45 Gy(RBE), patient 2: 0.08 Gy(RBE)), but never exceeded clinical tolerance doses. Additionally, slightly increased 1.1-weighted dose in healthy brain tissue was observed (patient 1: 0.81 Gy(RBE), patient 2: 0.53 Gy(RBE)). The variation of NTCP values due to variation of α/β from 2 to 3 Gy was much smaller for DDopt (2 percentage points (pp)) than for RefPlans (5 pp).

Conclusions: The novel dirty and clean dose concept allows for creating biologically more robust proton treatment plans with a more photon-like

dose response. The reduced uncertainties in RBE can, therefore, mitigate uncertainties introduced by using photon-based tolerance doses for OAR.

1 | INTRODUCTION

In clinical practice, a constant proton relative biological effectiveness (RBE) of 1.1 is used to account for differences in cell killing between protons and photons.[1–3] By using this approximation of a constant RBE, photon dose threshold values for organs at risk (OAR) are also applied in proton therapy. However, in-vitro, in-vivo, and emerging clinical studies[4–9] indicate that the RBE depends on various biological and physical parameters, for example, the linear energy transfer (LET), and therefore varies along a clinical treatment field.[10,11] As the proton slows down, the LET and hence the RBE increases. This may result in an RBE higher than 1.1 and an increased biological effective dose particularly at the distal edge of a spread-out Bragg peak (SOBP).[12] Due to safety margins used in clinical practice, the distal edge of an SOBP is usually placed in normal tissue. That is, the use of an RBE of 1.1 and photon dose threshold values for OAR introduces uncertainties regarding the expected biological response. Therefore, the variation of the RBE along the proton track that remains unconsidered in clinical practice, increases the probability of side effects. Neglecting the variability of RBE may, therefore, lead to unexpected normal tissue complication probability (NTCP) in OAR adjacent to the target volume.[4–8,13,14]

Several methods have been introduced to incorporate the RBE variability into plan optimization. Some of them optimize physical parameters like the LET or the product of LET and dose. Most of them are using the dose- or track-averaged LET to consider the RBE variability during treatment plan optimization.[15–19] However, averaging the LET may be inadequate since the same averaged LET can result from different LET spectra that may lead to different biological effects.[20,21] Other methods optimize the RBE-weighted dose by applying a variable RBE (vRBE) model.[15–19,21–24] Most RBE models depend on specific biological parameters to characterize the radiosensitivity of the tissue. These biological parameters have large uncertainties especially for heterogeneous tissue.[25,26] Since the result of a direct vRBE-weighted dose optimization depends strongly on the chosen biological parameters as well as on the chosen RBE model, these results might have large uncertainties, too. As a potential alternative, a recent study[27] comparing different strategies to incorporate the RBE variability into plan optimization briefly introduced dirty dose optimization.

The novel dirty and clean dose concept allows for considering the variability of RBE without averaging of the LET and without the need for specific biological parameters. The idea is to create proton treatment plans with a photon-like dose response and thereby to reduce uncertainties connected to the use of photon tolerance doses for OAR. Practically, the dirty and clean dose concept divides the 1.1-weighted dose distribution in two parts. The first part, the "clean" dose, is the dose deposited by low-LET protons. This fraction of the 1.1-weighted dose can be considered as photon-like. The second part, the "dirty" dose, is the dose deposited by the remaining high-LET protons. For this dose fraction, the RBE might exceed 1.1 and might therefore lead to unexpected side effects. The sum of the dirty and clean dose in a voxel adds up to the 1.1-weighted dose used for treatment planning in this voxel. Reducing the dirty dose in critical OAR during plan optimization might allow for more favorable treatment plans in terms of vRBE and reduce the risk of unexpected side effects due to the application of photon dose threshold values for OAR. Hahn et al.[27] concluded in their study that a deep understanding of the dirty and clean dose concept and, particularly, the influence of the free parameters on the optimization results is crucial to fully exploit its potential. However, such understanding is currently lacking.

Therefore, the aim of this study is a detailed introduction and explanation of the novel dirty and clean dose concept as well as the evaluation of its properties by, first, visualizing clean as well as dirty dose for simple irradiation geometries and, second, assessing the benefits and risks of optimizing them in exemplary cranial patient cases.

2 | METHODS

2.1 | Dirty and clean dose concept and optimization

The dirty dose contains all dose contributions by individual protons with an LET above a defined LET threshold ($\text{LET}_{\text{thres}}$). The remaining low-LET dose contributions yield the clean dose, that is, the 1.1-weighted dose is the sum of the clean and dirty dose. The actual LET value of each individual proton in a voxel is considered

by a binary filter and there is no voxel-wise averaging of the LET spectrum. Note, that the ratio between clean and dirty dose depends on the chosen LET threshold.

Since the dirty dose (as well as the clean dose) distribution is just another dose distribution, it can be optimized in the same way as any other dose distribution. All objectives usable for standard dose optimization (max dose, min dose, uniform dose, …) can also be applied on clean and dirty dose distributions. However, in contrast to standard dose optimization, two parameters must be chosen when applying dirty dose optimization objectives. First, the LET threshold parameter, which defines the part of the dose distribution to be considered as dirty dose and, second, the dirty dose level parameter defining the dose objective used on this dirty dose distribution. For example, when using the max dirty dose objective, the following parameters must be chosen:

a) LET threshold: only protons with an LET higher than this value contribute to the dirty dose and are considered during optimization of dirty dose and
b) max dirty dose level: maximum allowed dirty dose value in a voxel, dirty dose in a voxel exceeding this value gets penalized during optimization.

In this work, standard dose optimization was extended by adding dirty dose optimization. In dose-limiting OAR close to the target volume, dose contributions from high-LET protons (above the LET_{thres}) that exceeded a defined maximum dose level (max dirty dose) were penalized during optimization. Therefore, the max dirty dose objective acts similarly to the standard max dose objective, but only on one part of the dose distribution: the dirty dose distribution. A method to score clean and dirty dose distributions was implemented as a binary filter together with the dose scorer in the research version of the treatment planning system RayStation 11B-IonPG (RaySearch Laboratories AB, Stockholm, Sweden) and used to study and optimize dirty and clean dose distributions. The separation in dirty and clean dose is done during the actual simulation of the particle transport and not as a post-processing operation. When a particle traverses a voxel, the LET of this particle is calculated. If the LET is above LET_{thres}, the deposited dose by the particle is added to the dirty dose, otherwise the dose is added to the clean dose. For optimization a quadratic penalty function, as applied for standard dose optimization, is used.

2.2 | Two-step planning approach

A two-step planning approach was used to optimize different dirty dose distributions in a water phantom as well as in cranial patient cases (Figure 1). In a first step,

a clinical acceptable treatment plan fulfilling clinical goals for target dose coverage and OAR sparing was created. For this plan only standard dose objectives related to the 1.1-weighted dose were used. Therefore, this plan represented the optimal 1.1-weighted dose distribution and served as the reference plan (RefPlan) in this study. In a second step, dirty dose optimized treatment plans (DDopt) were created by maintaining all clinical plan configurations (number and orientations of all fields) and standard dose objective of the RefPlan and adding one additional MaxDirtyDose objective for each critical OAR. Since the fraction of dose considered as dirty depends on the LET_{thres}, the max dirty dose level for optimization was chosen as a percentage of the near-maximum dirty dose (DD_1, dirty dose that 1% of the volume receives) of the RefPlan in the respective OAR. That is, for a given LET_{thres} first, the DD_1 value of the regarded OAR in the RefPlan was calculated and then, the max dirty dose level in the DDopt plan was set relative to this DD_1 value (e.g., 50% of DD_1).

2.3 | Water phantom analysis

In-silico analyses using simple water phantoms were performed to illustrate the dirty and clean dose concept and the variation of these dose distributions as a function of the applied LET threshold. First, only one field, which homogeneously covers a 5 cm × 5 cm × 5 cm target volume in water, was studied (Figure 2a). A 1.1-weighted dose of 60 Gy(RBE) and 2 Gy(RBE) per fraction was prescribed to the target volume. Dirty dose distributions were scored for different LET threshold values and compared with other physical quantities, such as 1.1-weighted dose or proton dose-averaged LET (LET_d). For all comparisons with the vRBE-weighted dose, the Wedenberg RBE model[15] was applied with $\alpha/\beta = 2$ Gy and the voxel-wise proton dose per fraction.

Subsequently, a clinically more relevant scenario was studied by adding a 5 cm × 5 cm × 2.5 cm OAR adjacent to the same target volume in the water phantom (Figure 2c) to find suitable ranges for the LET threshold and dirty dose level of the max dirty dose objective. A reference plan with two orthogonal proton fields using only standard dose objectives and fulfilling clinical goals for target coverage and OAR sparing was created. Then, multiple dirty dose optimized plans using the two-step planning approach described above for different LET threshold and max dirty dose level combinations were created. Tested LET threshold values were between 1 and 4 keV/µm. A total of 28 dirty dose optimized plans with different LET_{thres}—max dirty dose level combinations were created and analyzed. In this way, suitable parameter ranges for the LET threshold and the max dirty dose level can be identified and afterwards applied for cranial patient cases. A tolerance dose of 54 Gy(RBE) was assumed for the
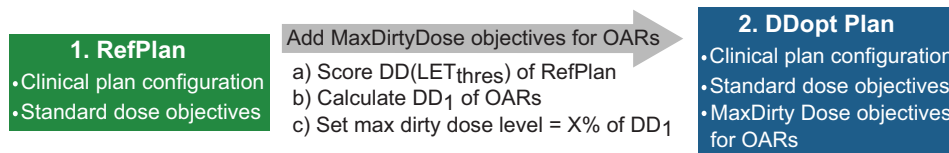
FIGURE 1 Two-step planning approach for creating the dirty dose optimized (DDopt) treatment plans by adding for each organ at risk (OAR). (A) MaxDirtyDose objective to the reference plan (RefPlan). DD, Dirty dose; DD_1, dirty dose that 1% of the volume receives; LET_{thres}, Linear energy transfer threshold.
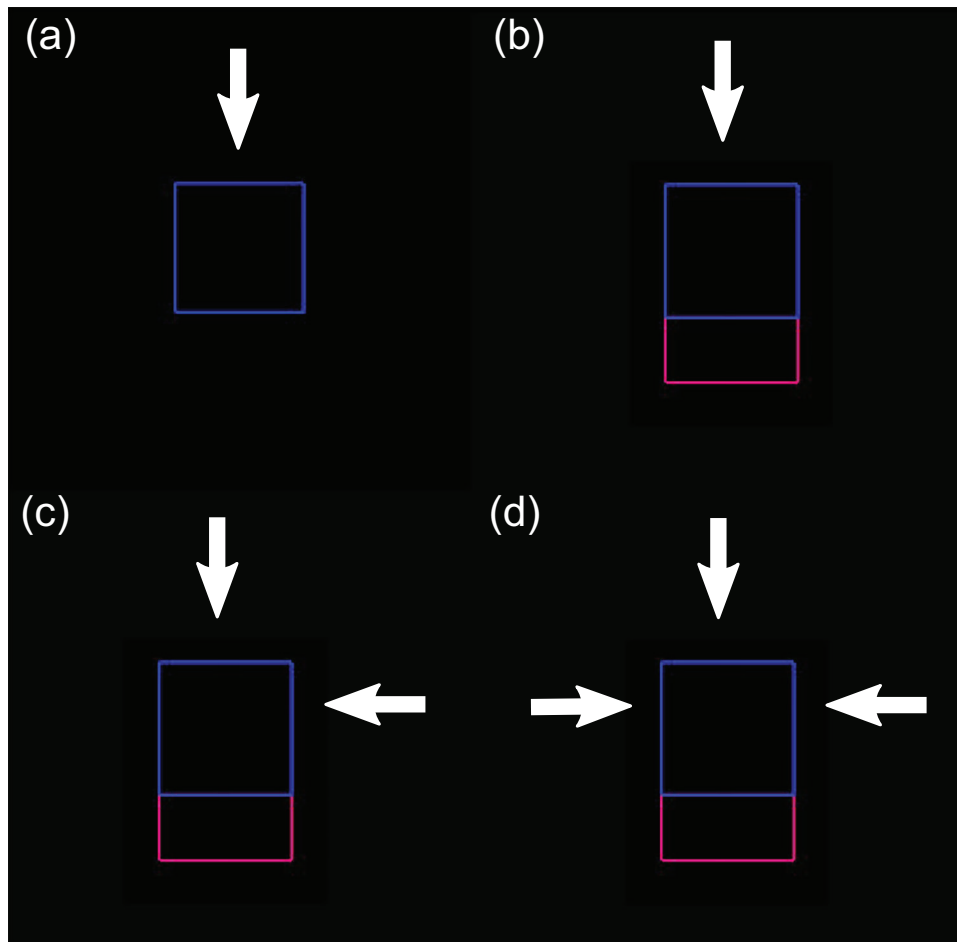

FIGURE 2 Computed tomography (CT) slices of the water phantom (25 cm × 25 cm × 25 cm) with target volume (blue, 5 cm × 5 cm × 5 cm) and organ at risk (magenta, 5 cm × 5 cm × 2.5 cm) used for visualization (a) and optimization (b–d) of dirty dose. The arrows indicate the beam orientations. The entire CT consists of water.

OAR. In order to evaluate the results of the dirty dose optimization, the dose-averaged LET and the vRBE-weighted dose distribution using the Wedenberg RBE model with $\alpha/\beta = 10$ Gy in the target volume and 2 Gy otherwise as well as the voxel-wise proton dose per fraction were calculated. For these calculations, the dose-averaged LET considering all protons in the local medium normalized to unity density was dertermined.[28]

To study the influence of the number of fields on the resulting dose distribution, we created DDopt plans with the same LET_{thres} (2 keV/µm) and the same max dirty dose level (70% of DD_1 of the RefPlan) using one (Figure 2b), two (Figure 2c), and three (Figure 2d) treatment fields.

2.4 | Patient analysis

To analyze potential benefits and risks when using dirty dose optimization, two representative patient cases

with cranial tumors were selected, both typical for proton beam therapy indications. The patients enrolled in a prospective registry study ("ProReg", German Clinical Trial Register: DRKS00004384) covered by ethics approval and had provided written informed consent. Patient 1 suffered from a meningioma of the base of skull receiving a prescribed dose of 54 Gy(RBE) in 30 fractions. Patient 2 was diagnosed with a chondrosarcoma and received a prescribed dose of 69.3 Gy(RBE) to the smaller clinical target volume CTV2 and 54.45 Gy(RBE) to the CTV1 in 33 fractions within simultaneous integrated boost strategy. For both patients, dose-limiting OAR close to the target volume were brainstem, chiasm, right and left optical nerve. Clinically acceptable multi-field optimized pencil beam scanning planning target volume-based treatment plans served as reference plans (RefPlan). All reference plans included only objectives based on the 1.1-weighted dose and represent therewith the optimal absorbed dose distribution.

To create the dirty dose optimized plans (DDopt), the above described two-step planning approach was used and a max dirty dose objective for each dose-limiting OAR was added to the standard dose objectives of the RefPlan. Combinations of LET threshold and dirty dose level yielding the best results in the prior water phantom studies were used to create a set of different DDopt plans. For each patient a total of nine DDopt treatment plans were created. Like in the water phantom studies, the max dirty dose level for a set LET threshold was chosen as a percentage of the DD_1 found in the RefPlan in the regarded OAR for the same LET threshold.

For each plan, the resulting 1.1-weighted dose distribution ($D_{1.1}$), the LET_d distribution and the vRBE-weighted dose distribution using the Wedenberg RBE model (D_{wed}) as well as the based on the $D_{1.1}$ resulting NTCP ($NTCP_{1.1}$) and the on the D_{wed} based NTCP ($NTCP_{wed}$) were obtained to analyze the potential benefits and risks of the dirty and clean dose concept for the patient. If not stated otherwise, α/β = 10 Gy for the target volume and 2 Gy elsewhere as well as the voxel-wise proton dose per fraction were used when applying the Wedenberg RBE model. $NTCP_{wed}$ values based on the vRBE-weighted dose D_{wed} were calculated using the relative seriality model for brainstem necrosis (model parameters: s = 1, γ = 2.4, D50 = 65.1 Gy(RBE)) and blindness (s = 1, γ = 2.5, D50 = 65.0 Gy(RBE)).[29,30] The same $NTCP_{wed}$ calculations were repeated with an α/β = 3 Gy in healthy tissue including the critical OAR to estimate the influence of biological parameters. To evaluate the impact of the dirty dose optimization on the dose in the target volume the dose coverage (dose to 95% of the target volume $D_{95\%}$), the homogeneity index (HI) and the conformity index (CI) were calculated and compared to the reference plan. For all analyses, a dose and LET_d grid size of $2 \times 2 \times 2$ mm^3 and a statistical Monte Carlo uncertainty of 0.5% was used.
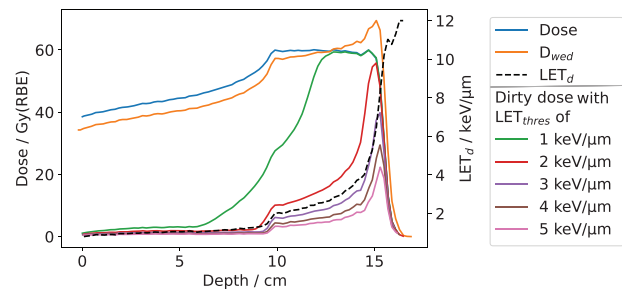

FIGURE 3 Line doses of the 1.1-weighted dose (Dose), Wedenberg dose (D_{wed}), and dirty dose distributions for different linear energy transfer threshold values (LET_{thres}) as well as dose-averaged LET_d in a clinical spread-out Bragg peak homogenously irradiating a target volume in a waterphantom (Figure 2a).

For each patient one LET-optimized (LETopt) treatment plan reducing LET_d values in all critical OAR higher than 2.5 keV/µm in voxels receiving a dose of at least 40 Gy(RBE) were created, to evaluate and compare the achieved optimization results by DDopt.

3 | RESULTS

3.1 | Water phantom analysis

The dirty dose distribution depended on the chosen LET threshold. Figure 3 shows the dirty dose distribution as a function of LET_{thres} between 1 and 5 keV/µm for an SOBP in water. Note that the peak of the dirty dose distribution closely resembles the peak of the D_{wed} distribution for LET_{thres} > 1 keV/µm and that the dirty dose distribution converges to the 1.1-weighted dose distribution when LET threshold goes to 0 keV/µm. Accordingly, the two-field reference plan in a water phantom with one target volume and one OAR showed increasing dirty dose at the distal edges of each beam, resulting in a dirty dose maximum at the position where the distal edges of the two fields overlap (Figure 4). In inverse proportion to the increase of the dirty dose, the clean dose decreased at the distal edges.

All tested combinations of LET threshold and max dirty dose level for optimization resulted in plans with a reduced near-maximum Wedenberg dose, $D_{wed,1}$, in the OAR (Figure 5b). The extent of this reduction in $D_{wed,1}$ depended on the chosen optimization parameter combination. For low LET_{thres} (~1 keV/µm), almost all the dose was considered, that is, optimized in dirty dose optimization. Then, the dirty dose objective acted similarly to a standard dose objective that optimizes the absorbed dose (Figure 5c) and not the LET (Figure 5a). The higher the LET threshold values, the smaller the part of the dose distribution considered in dirty dose optimization (Figure 3). Accordingly, the achievable reduction in vRBE-weighted dose became
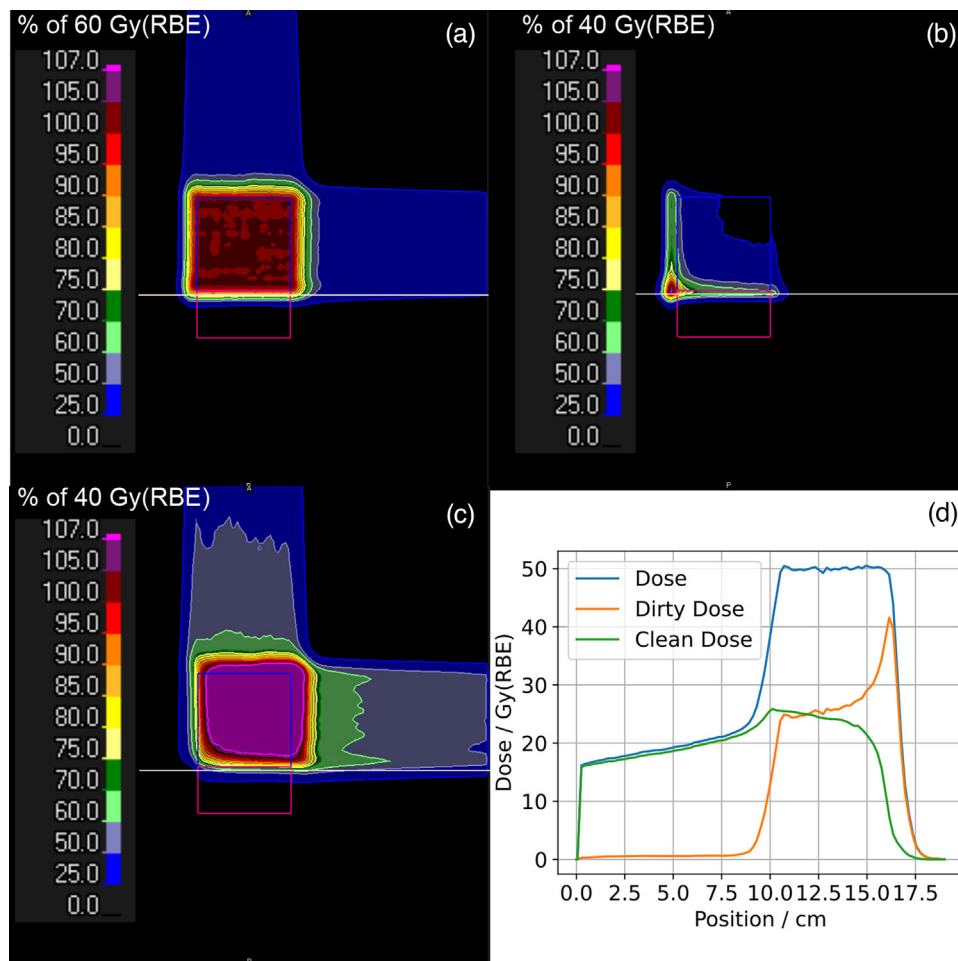
FIGURE 4 Representative computed tomography (CT) slice of the water phantom showing the target volume (blue) and the organ at risk (magenta) and dose distributions for the two-field reference plan: (a) 1.1-weighted dose distribution normalized to 60 Gy(RBE), (b) dirty dose distribution (LET threshold = 2.5 keV/μm), (c) clean dose distribution both normalized to 40 Gy(RBE). Corresponding line doses (d) along the horizontal grey line in the CT slice.

smaller. Furthermore, dirty dose optimization could lead to a (small) increase of the absorbed dose in the OAR (increase in $D_1 \leq 0.1$ Gy), even though the resulting vRBE-weighted dose $D_{wed,1}$ decreased in the OAR.

Some dirty dose optimization parameter combinations, especially the one achieving the highest $D_{wed,1}$ reduction, led, in some areas outside of the OAR (where no dirty dose objective was applied), to an increase in local dose by up to 25% compared to the corresponding RefPlan (Figure 6a, b). However, there was a range of parameter values (LET$_{thres}$ between 2 and 3.5 keV/μm, max dirty dose level between 60% and 70% of $DD_{1,RefPlans}$) in which a reduction of $D_{wed,1}$ was possible without a relevant change in the dose distribution relative to the reference plan (Figure 6c, d). For the latter plans, the reduction in vRBE-weighted dose in the OAR was mainly achieved by changing the LET distribution in the OAR but not the 1.1-weighted dose.

The comparison between DDopt plans with different numbers of treatment fields showed, in general, a decreasing amount of dose considered as dirty with an increasing number of treatment fields (Figure 7). Independent of the number of treatment fields a substantial reduction of the DD_1 in the OAR was achieved, namely, by 11.1 Gy(RBE), 11.8 Gy(RBE), and 10.8 Gy(RBE) for one, two, and three beam angles, respectively. For two and three treatment fields, the dirty dose reduction in the OAR led to an increased dirty dose in normal tissue areas, where no dirty dose objective was applied, by 0.2 Gy(RBE) and 1.3 Gy(RBE) for two and three treatment fields, respectively. For the one-field plan, the DD_1 in the normal tissue was slightly decreased by 0.1 Gy(RBE). In the latter case, the reduction of the near-maximum DD_1 in the OAR was achieved by redistributing the dirty dose within the OAR, which led to an increase in mean dirty dose in the OAR by 4.7 Gy(RBE). The two- and three-field configurations, on the other hand, reduced the mean dirty dose in the OAR by 1.2 Gy(RBE) and 1.8 Gy(RBE), respectively.
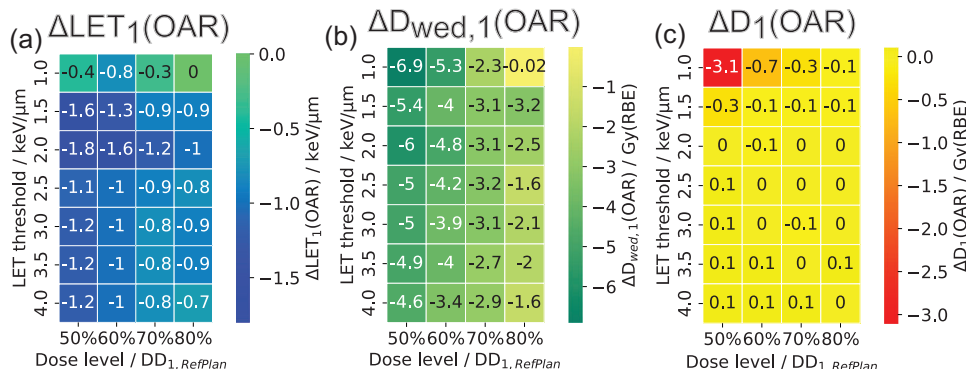
FIGURE 5 Differences between the dirty dose optimized plans and the reference plan for different combinations of linear energy transfer (LET) threshold and max dirty dose level used for dirty dose (DD) plan optimization in terms of near-maximum dose-averaged LET, $LET_{d,1}$, (a) near-maximum variable RBE-weighted dose $D_{wed,1}$, (b) and near-maximum 1.1-weighted dose D_1, (c) in the organ at risk.
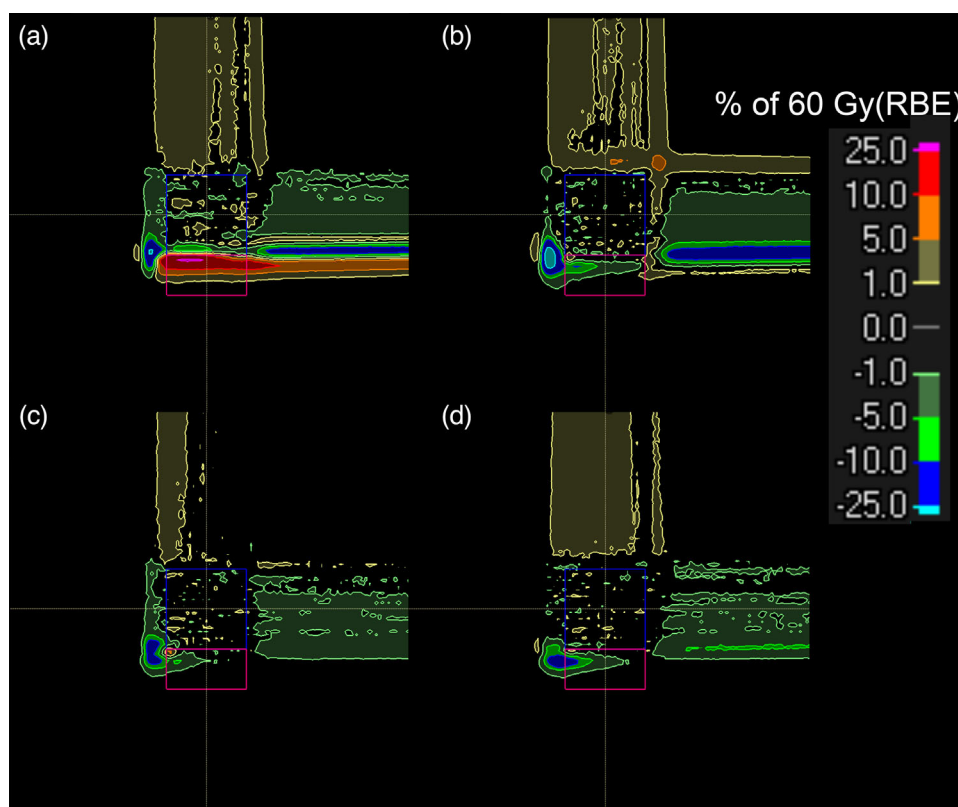

FIGURE 6 Differences in 1.1-weighted dose between the reference plan and four dirty dose (DD) optimized plans using different optimization parameter combinations (LET threshold, DD level in the OAR relative to reference plan). (a) (1 keV/μm, 50% × DD_1); (b) (2 keV/μm, 50% × DD_1); (c) (2 keV/μm, 70% × DD_1); (d) (2.5 keV/μm, 70% × DD_1). Contours of the target volume and the OAR in blue and magenta, respectively.

3.2 | Patient analysis

LET threshold values of 1.5, 2, and 2.5 keV/μm yielded the best results in the prior waterphantom studies and were, therefore, considered in the patient analysis together with max dirty dose levels of 40%, 50%, and 60% of the respective DD_1 values in the RefPlan. The computational time for scoring the dirty dose in addition to the standard 1.1-weighted dose was about 40% higher than for scoring only the 1.1-weighted dose. The optimization of the DDopt treatment plans took about 30% more time than the optimization of the RefPlans. All DDopt patient plans showed an increase in photon-like clean dose and at the same time a decrease in the dirty fraction of the dose in the OAR. Figure 8 shows this behavior exemplary for the chiasm of patient 1.
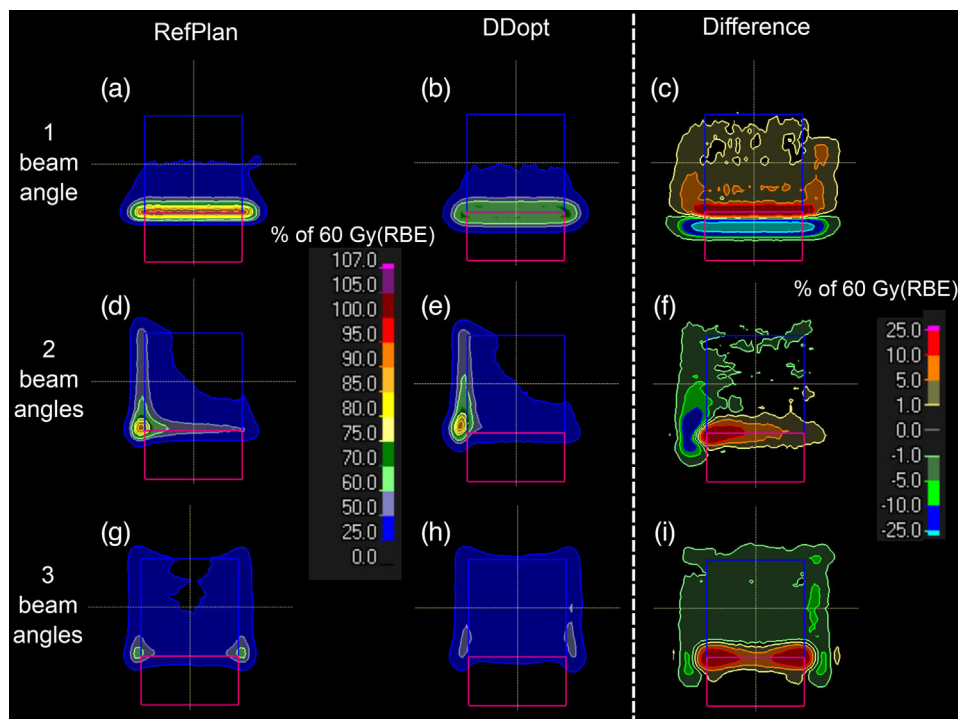
FIGURE 7 Dirty dose (DD) distributions for reference plans (RefPlan, a, d, g) and dirty dose optimized plans (DDopt, b, e, h) for one (a, b), two (d, e) and three (g, h) treatment fields as well as the difference between the DD of the RefPlans and the DDopt plans (c, f, i). The LET threshold was set to 2 keV/μm and the max dirty dose level to 70% of DD1 of the RefPlan. Contours of the target volume and the OAR in blue and magenta, respectively.

Results for patient 2 can be found in the supplement (Figure S1, S2). For all tested combinations of LET threshold and dose objective level, the dirty dose optimization led to slightly higher near-maximum values of the absorbed dose D_1 in the critical OAR. At the same time, all DDopt plans showed lower LET_d values and therefore a reduction of the near-maximum value of the Wedenberg dose $D_{wed,1}$ in all critical OAR. Figure 9a and B shows the results exemplary for the chiasm of patient 1. Only DDopt plans with the highest tested max dirty dose level (60% DD_1 of RefPlan) for patient 2 did not lead to a reduction of $D_{wed,1}$. The achieved reduction in variable RBE-weighted dose showed a more pronounced dependence on the chosen dose level than on the LET threshold (Figure 9).

Dirty dose optimization did not impact the dose distribution of the target volume. All DDopt plans showed the same HI and CI as the corresponding RefPlan. For patient 1, the mean difference (±standard deviation) of the $D_{95\%}$ in the CTV between the DDopt plans and the corresponding RefPlan was 0.04 (±0.10) Gy(RBE). For patient 2 this difference was 0.06 (±0.01) Gy(RBE) for CTV1 and 0.02 (±0.37) Gy(RBE) for CTV2, respectively. However, dirty dose optimization slightly increased the absorbed dose in the OAR (Figure 9c) and led to an increase of the mean absorbed dose to healthy brain tissue (Figure 9d). The increase in 1.1-weighted

D_1 (±standard deviation) in the OAR averaged over all DDopt plans and all OAR compared to the RefPlan was 0.47 (±0.65) Gy(RBE) and 0.08 (±0.28) Gy(RBE) for patient 1 and 2, respectively. This increase translated into a maximum increase of the $NTCP_{1.1}$ of 1 percentage point (pp). The average increase of mean 1.1-weighted dose in healthy brain tissue compared to the RefPlan was 0.81 (±0.21) Gy(RBE) and 0.53 (±0.20) Gy(RBE) for patient 1 and 2, respectively.

For patient 1 and compared to the DDopt plans, the LETopt plan showed an overall higher reduction in both LET_d and D_{wed} in the critical OAR, including the near-maximum values LET_1 and $D_{wed,1}$. Averaged over all DDopt plans, LET_1 and $D_{wed,1}$ in the chiasm were 4.06 (±0.49) keV/μm and 56.98 (±1.05) Gy(RBE), respectively. For the LETopt plan, values of 3.95 keV/μm and 51.71 Gy(RBE) were found for LET_1 and $D_{wed,1}$, respectively. The corresponding vRBE-weighted dose and LET volume histograms for an exemplary DDopt and the LETopt plan can be found in the supplement (Figure S4). Besides reducing the vRBE-weighted dose in OAR, LETopt also influenced the dose in the target volume and the healthy brain tissue leading to values of 52.64 Gy(RBE) and 7.04 Gy(RBE) for $D_{95\%}$ of the CTV and D_{mean} of the healthy brain tissue, respectively. DDopt plans showed an averaged $D_{95\%}$ for the CTV of 53.04 (±0.10) Gy(RBE) and an averaged
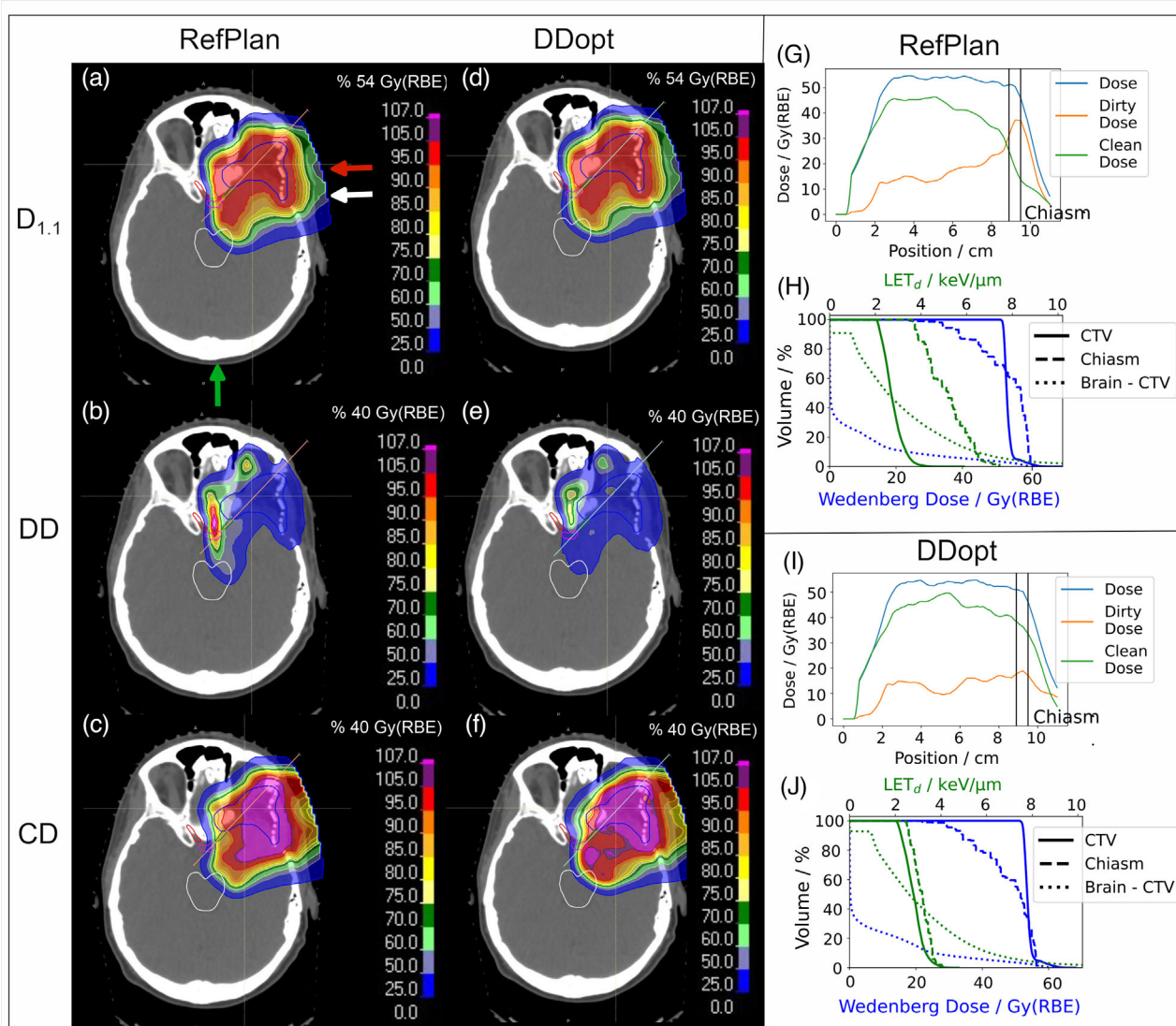
FIGURE 8 Representative slice for patient 1 including the CTV (blue), brainstem (white), chiasm (magenta), right (green) and left (red) optical nerve and overlaying the 1.1-weighted dose ($D_{1.1}$), dirty dose (DD) and clean dose (CD) for the reference plan RefPlan (a, b, c) and the dirty dose optimized plan DDopt (d, e, f) with LET threshold = 2 keV/μm and max dirty dose level = 50%. Corresponding line dose profiles (along the indicated straight lines) for the reference plan (g) and the dirty dose optimized plan in (i) as well as dose-volume histograms using the Wedenberg RBE model (blue) and linear energy transfer-volume histograms (green) for the reference plan (h) and the dirty dose optimized plan (j). Arrows indicate coplanar (white) and non-coplanar (red) beams as well as beams passing through the skull cap (green).

D_{mean} for healthy brain tissue of 6.65 ($\pm$0.21) Gy(RBE). When comparing the LETopt plan with the corresponding RefPlan, the LETopt plan achieved a ΔLET_1 of -3.35 keV/μm and a $\Delta D_{wed,1}$ of -8.03 Gy(RBE) for the chiasm of patient 1. Compared to the RefPlan, LETopt reduced the CI and HI by 0.03 and 0.04, respectively, and the $D_{95\%}$ for the CTV by 0.44 Gy(RBE). Furthermore, the mean dose in healthy brain tissue was increased by 1.2 Gy(RBE). For patient 2, the results for DDopt and LETopt were found to be comparable. For the brainstem, the LETopt plan achieved ΔLET_1 and $\Delta D_{wed,1}$ values of -2.61 keV/μm and -1.1 Gy(RBE), respectively. Compared to the RefPlan, HI and CI values of

the LETopt plan remained unchanged. The difference of $D_{95\%}$ of the target volume between the RefPlan and the LETopt plan was -0.05 Gy(RBE) for CTV1 and 0.02 Gy(RBE) for CTV2, respectively. The mean dose to healthy brain tissue was increased by 0.62 Gy(RBE). For both patients, vRBE-weighted dose-volume histograms using the Wedenberg RBE model and LET-volume histograms of the LETopt plans can be found in the supplement (Figure S3).

All DDopt plans reduced the $NTCP_{wed}$ in all OAR compared to the corresponding RefPlan when considering the Wedenberg dose (Table 1). Furthermore, varying α/β from 2 to 3 Gy led to less difference in $NTCP_{wed}$
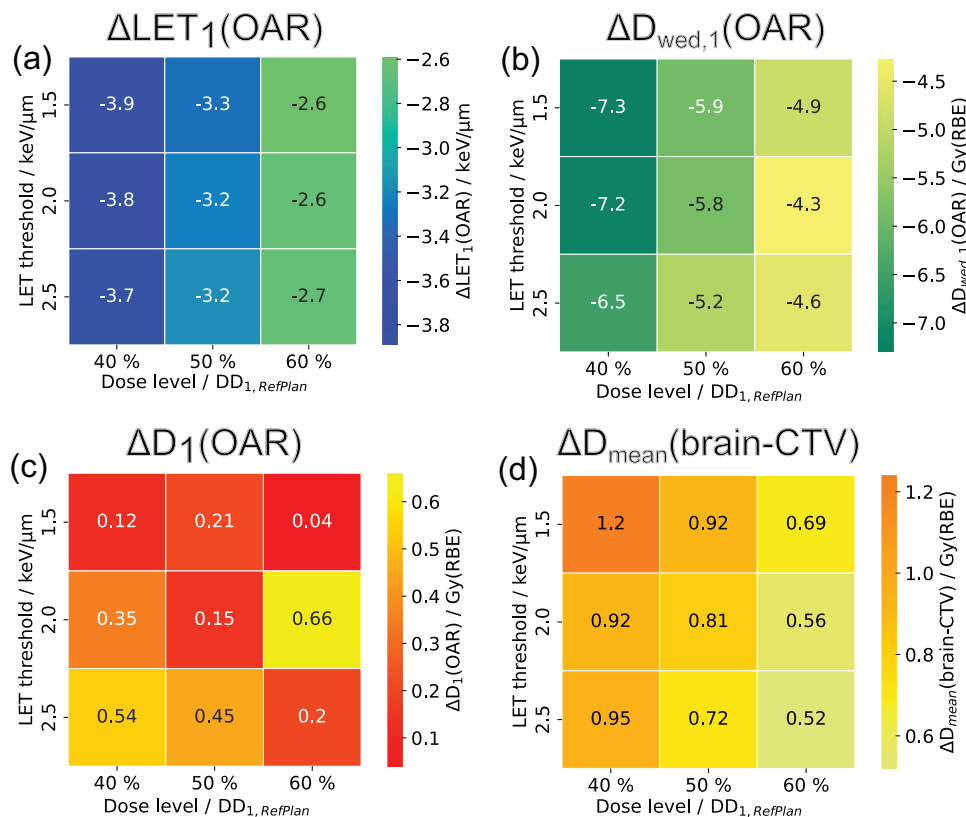
FIGURE 9 Differences between the dirty dose optimized plans and the reference plan for patient 1 in the chiasm: near-maximum dose-averaged linear energy transfer (LET), $LET_{d,1}$ (a), near-maximum variable relative biological effectiveness (RBE)-weighted dose using the Wedenberg RBE model, $D_{wed,1}$ (b), near-maximum absorbed dose, D_1, (c). Differences in mean dose in the healthy brain tissue, D_{mean} (d).

TABLE 1 $NTCP_{wed}$ values resulting from the variable relative biological effectiveness (RBE)-weighted dose distribution using the Wedenberg RBE model for the reference plan (RefPlan) and dirty dose optimized plans (DDopt).

Organ at risk	α/β/Gy	Patient 1		Patient 2	
		RefPlan	DDopt	RefPlan	DDopt
Brainstem	2	1%	0% $\pm$ 0%	17%	11% $\pm$ 2%
	3	0%	0% $\pm$ 0%	12%	8% $\pm$ 1 %
Chiasm	2	20%	4% $\pm$ 2%	18%	6% $\pm$ 1%
	3	12%	2% $\pm$ 2%	13%	5% $\pm$ 1%
Right optical nerve	2	0%	0% $\pm$ 0%	18%	7% $\pm$ 2%
	3	0%	0% $\pm$ 0%	12%	5% $\pm$ 1%
Left optical nerve	2	27%	12% $\pm$ 3%	6%	2% $\pm$ 2%
	3	18%	8% $\pm$ 5%	4%	1% $\pm$ 1%

Note: For DDopt, the mean $NTCP_{wed}$ and standard deviation for all considered dirty dose optimization parameter combinations are given.

(defined as $\Delta NTCP_{wed} = NTCP_{wed}(\alpha/\beta = 2$ Gy)— $NTCP_{wed}(\alpha/\beta = 3$ Gy)) for all DDopt plans. For the RefPlans of patient 1 and 2, the mean $\Delta NTCP_{wed}$ averaged over all OAR was 5 ($\pm$3) pp and 5 ($\pm$2), respectively. For the DDopt plans, the same variation in α/β led to a smaller mean $\Delta NTCP_{wed}$ of 2 ($\pm$2) pp and 2 ($\pm$1) pp for patient 1 and 2, respectively. The relative changes of $NTCP_{wed}$ (defined as $\Delta NTCP_{wed}/NTCP_{wed}(\alpha/\beta = 2$ Gy) for OAR with $NTCP_{wed}(\alpha/\beta = 2$ Gy) > 0) averaged over all

OAR were comparable for the RefPlans and the DDopt plans and were in the order 0.5 and 0.3 for patient 1 and 2, respectively (Table 1).

4 | DISCUSSION

The basic idea of the novel dirty and clean dose concept is to separate the 1.1-weighted proton dose

contributions into a clean dose part with an expected biological dose response similar to that of photons and a dirty dose part with a non-photon-like dose effect. The goal of the concept is to decrease the dirty dose in critical OAR to reduce the RBE-related uncertainties when using photon-based OAR tolerance dose values in proton therapy plan optimization and approval together with a constant RBE.

When applying the dirty and clean dose concept, values for two parameters, namely, the LET threshold and the dirty dose level, are decisive and must be chosen for optimization. The present analysis showed, as expected from the definition of the novel concept, that for low LET threshold values, almost the whole dose was considered as "dirty" and, consequently, the maximum dirty dose objective acted similarly to a standard dose objective in plan optimization. On the other hand, for too high LET threshold values, nearly no influence on the resulting plan was observed, because the optimized "dirty" part of the dose was too small. Accordingly, the choice of the LET threshold determines whether the dose distribution is changed, or the LET is redistributed to achieve the reduction of the dirty dose. Moreover, the choice of the max dirty dose level showed a greater impact on the resulting plan than the LET threshold value. In the performed water phantom studies, LET threshold values between 1.5 and 2.5 keV/µm resulted in the best results, that is, the most pronounced reduction in vRBE dose in the OAR. Studies[4,31–35] analyzing the occurrence of unexpected side effects after proton therapy found radiation-induced image changes to occur in voxels especially with a mean LET higher than 2.5 keV/µm. It should be noted that these studies considered dose- or track-averaged LET values in their analysis. Moreover, according to the Wedenberg RBE model an LET of 1.5 keV/µm leads to an RBE of 1.1 when using an $\alpha/\beta = 2$ Gy and a dose per fraction of 2 Gy. Therefore, this value might be suitable for dividing the 1.1-weighted dose into a clean and a dirty part.

We calculated the LET_d and the vRBE-weighted dose using the Wedenberg RBE model to assess the benefits and risks of the dirty and clean dose concept. Although averaging the LET_d might introduce uncertainties,[36] most biological data and analyses of clinical outcome data are based on averaged LET_d values.[4–6,9] This might change in the future since the amount of microdosimetry studies analyzing LET spectra and LET values of individual particles is increasing[21,36–38] and new techniques for calculating these quantities have been developed.[39,40] Nevertheless, since biological analyses and correlations of clinical outcome data with LET spectra and other microdosimetric quantities are still lacking, we chose to calculate the LET_d and vRBE-weighted dose distribution using the Wedenberg RBE model to assess the benefits of the novel concept. In this way, also a comparison with other strategies to optimize vRBE-related quantities is possible since

most of these studies calculated similar quantities to assess the benefits of their strategies. Using the dirty and clean dose optimization strategy led to more beneficial plans in terms of vRBE using the Wedenberg RBE model. Most DDopt plans reduced the number of high LET protons, thereby reducing the LET_d and the near-maximum vRBE-weighted dose in critical OAR translating into lower $NTCP_{wed}$ values. Interestingly, for DDopt plans, both the variable RBE and $NTCP_{wed}$ values were less dependent on variations in the α/β-value compared with the corresponding reference plan. Especially, the resulting absolute changes in $NTCP_{wed}$ were clearly smaller for the DDopt plans compared to the Ref-Plans. This may be of relevance, since the uncertainty in the α/β value, which is needed to model RBE, is usually considered as a major source of uncertainty for variable RBE dose.[25,26] The decreased dependence of the NTCP on biological parameters can be explained with the dependence of the variable RBE on the α/β value. In the Wedenberg model, the term depending on α/β is multiplied with LET_d. Since the LET_d values in OAR are generally smaller in DDopt than in reference plans, a change of or an uncertainty in the α/β value also has less effect on the variable RBE and thus NTCP in DDopt plans.

Nevertheless, optimizing the dirty dose also comes at a cost. DDopt plans showed a higher absorbed dose in surrounding healthy tissue, where no dirty dose objective was applied. Furthermore, a small increase of the near-maximum 1.1-weighted dose in the critical OAR was observed, which translated in a small $NTCP_{1.1}$ increase by a maximum of 1 pp. However, the clinically used tolerance doses for the 1.1-weighted dose in the OARs were never exceeded and the resulting vRBE-weighted dose and, therefore, also the $NTCP_{wed}$, were still reduced. This may be due to the two-step planning approach used here. This approach is in line with other studies[17,27,41] analyzing potential optimization strategies. By adding the max dirty dose objective to the standard dose objectives of the reference plan to create the DDopt plans, the standard max dose objectives also restricted the maximum 1.1 weighted dose in the OAR for the DDopt plans. In this study, dirty dose optimization showed nearly no impact on the dose coverage, homogeneity, and conformity of the target volume, which is in line with current guidelines[1] suggesting to keep target dose the same when applying strategies for reducing vRBE related uncertainties in OAR.

When comparing the DDopt plans with the LETopt plans we found a slightly higher reduction of $D_{wed,1}$ in the OAR for the LETopt plans of patient 1. At the same time, the LETopt reduced the dose coverage, homogeneity, and conformity in the target volume, which might influence tumor control and might contradict current guidelines[1] suggesting to keep the dose distribution in the target volume unchanged while optimizing RBE related quantities in OAR. Adjusting the objectives of the

LETopt plan of patient 1 might prevent dose changes in the target volume but might at the same time reduce the achieved reduction of $D_{wed,1}$ and might therefore lead to comparable results between DDopt and LETopt, as found for patient 2. No influence on the dose in the target was found for DDopt for any of the tested parameter combinations. Hence, optimization of dirty dose appears less likely to result in dose changes in target volume compared to the optimization of LET_d.

We chose patients with typical cranial tumors to confirm the basic findings of the water phantom studies because their geometrical and anatomical conditions might result in especially high RBE uncertainties in normal tissues[42,43] and, consequently, most clinical evidence for a variable RBE in proton therapy is available for these entities. Therefore, patients with cranial tumors may benefit most from the novel dirty dose optimization strategy. Here, two patient cases with different prescribed doses were presented to show the feasibility of the concept for different dose regimes. In the future, larger in silico patient studies that go beyond introducing the dirty and clean dose concept could extend to various body sites and further confirm the obtained results in a more general way.

Several other strategies[44–48] have been proposed to account for vRBE uncertainties during plan optimization, for example, the optimization of the averaged LET, the track-end distribution, the product of dose times averaged LET and a direct optimization of vRBE-weighted dose using different RBE models. To be able to assess the efficiency of the different strategies some publications evaluated the same quantities as in the study at hand, so that a direct comparison is possible. Henjum et al.,[48] for example, optimized the vRBE-weighted dose using the Rørvik[21] and McNamara[16] RBE model. They achieved a reduction of about 3% of the maximum vRBE-weighted dose compared to a reference plan. With the dirty dose optimization in this study a reduction of the near-maximum vRBE-weighted dose of up to 11% was achieved. However, it should be noted that here the Wedenberg[15] RBE model was applied for vRBE-weighted dose calculation. When optimizing the track-end distribution Traneus and Ödén[44] found a reduction in $NTCP_{wed}$ of up to 19 pp, which was also achieved in this study with dirty dose optimization. Moreover, dirty dose optimization led to a reduction of the near-max LET_d of up to 4 keV/µm while Liu et al.,[46] for example, reported a reduction of up to approximately 2 keV/µm for the maximum value of LET_d in OAR when applying different strategies to optimize the dose-averaged LET_d. Strategies optimizing the LET or the product of dose and averaged LET usually optimize dose- or track-averaged LET. Therefore, they may introduce new uncertainties, since different LET spectra in a voxel with different biological effects, can lead to the same averaged LET value. Whether these uncertainties are negligible in a clinical environment is currently under debate. Some studies did not find a significant difference in proton RBE values based on averaged and not-averaged values,[49] while other studies suggest that the use of the actual LET value might be favorable.[36] With the dirty and clean dose optimization approach, the LET value of each proton determines whether this proton is considered in the optimization. Optimizing the product of dose and LET_d tend to overestimate the influence of the LET_d, since both quantities are included equally in the optimization. This means that a doubling of the LET_d leads to the same effect as a doubling of the dose. When optimizing a dirty dose distribution there are two free parameters (LET threshold and, e.g., max dirty dose level). With these parameters, one can choose which dirty dose distribution is optimized and thus (indirectly) influence in which ratio dose and LET are considered in the optimization. For a direct optimization of the vRBE-weighted dose, the choice of RBE model is crucial. For proton therapy, many different RBE models are described in the literature,[15–19,21–24] and most of them are based on cell survival data. So far, all these models are only used for research purposes and a clinically accepted RBE model for the use in proton treatment planning is still lacking. Moreover, the use of an RBE model requires accurate knowledge of biological parameters, such as α/β, which are typically uncertain. Since the dirty dose distribution is just another dose distribution, the optimization of this distribution corresponds to an optimization of purely physical parameters and was found to be more robust against uncertainties in α/β.

A recent study[27] compared four different strategies, including the optimization of dirty dose, that all achieved a vRBE-weighted dose reduction in critical OAR while maintaining plan quality regarding the 1.1-weighted dose. In that study, the choice of only a single dose level and LET threshold value was considered as the limiting factor to fully exploit the potential of DDopt. In the studies performed here, (especially, those with the water phantom) the range of suitable optimization parameters could be narrowed down to approximately 1.5–2.5 keV/µm for the LET threshold and 40%–60% of the DD_1 of the corresponding RefPlan for the max dirty dose level. In this range, the resulting DDopt plans were found to be robust against changes of the parameter values. The parameter combination used in the before mentioned study was within this range and can therefore, based on the results at hand, be considered as a suitable choice. Since the study mentioned before analyzed one plan for each of the ten patient cases studied, the results of the work at hand are expected to hold also for a larger patient cohort. For the future, probably the best approach to determine suitable optimization parameters would be the analysis of clinical outcome data aiming at max dirty dose level and LET threshold values that are associated with toxicities. As long as these data are not available, the two-step

planning approach suggested here (first, RefPlan and based on that, second, DDopt plan) might be a practical alternative.

In the current implementation, the separation in dirty and clean dose is performed only for primary and secondary protons. The dose of heavier secondary particles is treated as clean dose, since the uncertainties when calculating their LET spectra are currently under investigation. In a future implementation, the separation in clean and dirty dose will be performed for all particles, which might further improve the optimization results when applying the dirty and clean dose concept.

In this study, the same optimization weights as in the corresponding RefPlan were used in the DDopt plans. For the MaxDirtyDose objective a weight of around 10% of the weight of the standard dose objectives used for OAR sparing was applied. Therefore, the weights of all standard dose objectives, including the MaxDirtyDose objective, were kept constant. Studies using multi criteria optimization might be performed in the future to better understand the influence of the individual weights on the resulting dose distribution. Using other clean and dirty dose related objectives may further improve the optimization results in terms of the biological effect. For example, considering different dirty dose volume histogram parameters or the mean dirty dose in an OAR might help achieving treatment plans with a photon like dose response. Furthermore, comparing between different number of treatment fields, showed that the stopping protons might get redistributed to normal tissue outside of the OAR to achieve the desired reduction of dirty dose in the OAR. Therefore, future studies could add dirty and clean dose related objectives for the normal tissue also outside the OAR to prevent or at least limit large amounts of dirty dose somewhere in healthy tissue. As the dirty and clean dose concept just requires the optimization of another dose distribution, this concept allows for the implementation of all objectives used for standard dose optimization, as well as the implementation of robust optimization and robustness analysis in the same way as performed for the 1.1-weighted dose distribution.

5 | CONCLUSION

The dirty and clean dose concept separates the 1.1-weighted proton dose in two parts; the clean dose, with an expected biological dose response similar to that of photons and the dirty dose with a non-photon like dose response. It allows for a targeted optimization of the dirty part of the dose, which is more likely to contribute to RBE-related unexpected side effects in proton therapy. As a consequence, the biological effect of DDopt plans is expected to be more similar to photon irradiation and less uncertainties are introduced when applying dose

threshold values for OAR sparing based on photon data. In terms of the biological effect in critical OAR DDopt plans outperform, depending on the dose level and LET threshold, clinically acceptable RefPlans. The resulting NTCP values of DDopt plans were not only reduced but also more robust against the variation of uncertain biological model parameters.

CONFLICT OF INTEREST STATEMENT
Jakob Ödén and Erik Traneus are employed at Ray-Search Laboratories AB, Stockholm, Sweden. Erik Traneus is the inventor of patents EP3682945B1, EP3618924A1. The other authors report no conflict of interest.

REFERENCES
1. Paganetti H, Blakely E, Carabe-fernandez A, Carlson DJ, Held KD. Report of the AAPM TG-256 on the relative biological effectiveness of proton beams in radiation therapy. *Med Phys*. 2019;46(3):e53-e78. doi:10.1002/mp.13390
2. Paganetti H, Niemierko A, Ancukiewicz M, et al. Relative biological effectiveness (RBE) values for proton beam therapy. *Int J Radiat Oncol Biol Phys*. 2002;53(2):407-421. doi:10.1016/S0360-3016(02)02754-2
3. Heuchel L, Hahn C, Pawelke J, Sørensen BS, Dosanjh M, Lühr A. Clinical use and future requirements of relative biological effectiveness: survey among all European proton therapy centres. *Radiother Oncol*. 2022;172:134-139. doi:10.1016/J.RADONC.2022.05.015
4. Bahn E, Bauer J, Harrabi S, Herfarth K, Alber M. Late contrast enhancing brain lesions in proton-treated patients with low-grade glioma : clinical evidence for increased periventricular sensitivity and variable RBE. *Int J Radiat Oncol Biol Phys*. 2020;107(3):571-578. doi:10.1016/j.ijrobp.2020.03.013
5. Eulitz J, Troost EGC, Raschke F, et al. Predicting late magnetic resonance image changes in glioma patients after proton therapy. *Acta Oncol*. 2019;58(10):1536-1539. doi:10.1080/0284186X.2019.1631477
6. Peeler CR, Mirkovic D, Titt U, et al. Clinical evidence of variable proton biological effectiveness in pediatric patients treated for ependymoma. *Radiother Oncol*. 2016;121(3):395-401. doi:10.1016/j.radonc.2016.11.001
7. Engeseth GM, He R, Mirkovic D, et al. Mixed effect modeling of dose and linear energy transfer correlations with brain image changes after intensity modulated proton therapy for skull base head and neck cancer. *Int J Radiat Oncol Biol Phys*. 2021;111(3):684-692. doi:10.1016/j.ijrobp.2021.06.016
8. Underwood TSA, Grassberger C, Bass R, et al. Asymptomatic late-phase radiographic changes among chest-wall patients are associated with a proton RBE exceeding 1.1. *Int J Radiat Oncol Biol Phys*. 2018;101(4):809-819. doi:10.1016/j.ijrobp.2018.03.037
9. Eulitz J, Troost GCE, Klünder L, et al. Increased relative biological effectiveness and periventricular radiosensitivity in proton therapy of glioma patients. *Radiother Oncol*. 2023;178:109422. doi:10.1016/J.RADONC.2022.11.011
10. Paganetti H. Relative biological effectiveness (RBE) values for proton beam therapy. Variations as a function of

biological endpoint, dose, and linear energy transfer. *Phys Med Biol*. 2014;59(22):R419. doi:10.1088/0031-9155/59/22/R419

11. Paganetti H. Mechanisms and review of clinical evidence of variations in relative biological effectiveness in proton therapy. *Int J Radiat Oncol Biol Phys*. 2022;112(1):222-236. doi:10.1016/J.IJROBP2021.08.015

12. Lühr A, von Neubeck C, Krause M, Troost EGC. Relative biological effectiveness in proton beam therapy—Current knowledge and future challenges. *Clin Transl Radiat Oncol*. 2018;9:35-41. doi:10.1016/j.ctro.2018.01.006

13. Wang CC, McNamara AL, Shin J, et al. End-of-range radiobiological effect on rib fractures in patients receiving proton therapy for breast cancer. *Int J Radiat Oncol Biol Phys*. 2020;107(3):449-454. doi:10.1016/j.ijrobp.2020.03.012

14. Harrabi SB, von Nettelbladt B, Gudden C, et al. Radiation induced contrast enhancement after proton beam therapy in patients with low grade glioma—How safe are protons? *Radiother Oncol*. 2021;167:211-218. doi:10.1016/J.RADONC.2021.12.035

15. Wedenberg M, Lind BK, Hårdemark B. A model for the relative biological effectiveness of protons: the tissue specific parameter α/β of photons is a predictor for the sensitivity to LET changes. *Acta Oncol*. 2013;52(3):580-588. doi:10.3109/0284186X.2012.705892

16. Mcnamara AL, Schuemann J, Paganetti H. A phenomenological relative biological effectiveness (RBE) model for proton therapy based on all published in vitro cell survival data A phenomenological relative biological effectiveness (RBE) model for proton therapy based on all published in vitro. *Phys Med Biol*. 2015;60:8399-8416. doi:10.1088/0031-9155/60/21/8399

17. Unkelbach J, Botas P, Giantsoudi D, Gorissen BL, Paganetti H. Reoptimization of intensity modulated proton therapy plans based on linear energy transfer. *Int J Radiat Oncol Biol Phys*. 2016;96(5):1097-1106. doi:10.1016/J.IJROBP.2016.08.038

18. Wilkens JJ, Oelfke U. A phenomenological model for the relative biological effectiveness in therapeutic proton beams. *Phys Med Biol*. 2004;49(13):2811. doi:10.1088/0031-9155/49/13/004

19. Mairani A, Dokic I, Magro G, et al. A phenomenological relative biological effectiveness approach for proton therapy based on an improved description of the mixed radiation field. *Phys Med Biol*. 2017;62(4):1378-1395. doi:10.1088/1361-6560/AA51F7

20. Guan F, Peeler C, Bronk L, et al. Analysis of the track- and dose-averaged LET and LET spectra in proton therapy using the geant4 Monte Carlo code. *Med Phys*. 2015;42(11):6234-6247. doi:10.1118/1.4932217

21. Rørvik E, Thornqvist S, Stokkevag CH, Dahle TJ, Fjæra LF, KS Ytre-Hauge. A phenomenological biological dose model for proton therapy based on linear energy transfer spectra. *Med Phys*. 2017;44(6):2586-2594. doi:10.1002/MP.12216

22. Belli M, Campa A, Ermolli I. A semi-empirical approach to the evaluation of the relative biological effectiveness of therapeutic proton beams: the methodological framework. *Radiat Res*. 1997;148(6):592-598. doi:10.2307/3579735

23. Chen Y, Ahmad S. Empirical model estimation of relative biological effectiveness for proton beam therapy. *Radiat Prot Dosimetry*. 2012;149(2):116-123. doi:10.1093/RPD/NCR218

24. Jones B. Towards achieving the full clinical potential of proton therapy by inclusion of LET and RBE models. *Cancers*. 2015;7(1):460-480. doi:10.3390/CANCERS7010460

25. Paganetti H. Relating the proton relative biological effectiveness to tumor control and normal tissue complication probabilities assuming interpatient variability in α/β. *Acta Oncol*. 2017;56(11):1379-1386. doi:10.1080/0284186X.2017.1371325

26. McMahon SJ. Proton RBE models: commonalities and differences. *Phys Med Biol*. 2021;66(4):04NT02. doi:10.1088/1361-6560/abda98

27. Hahn C, Heuchel L, Ödén J, et al. Comparing biological effectiveness guided plan optimization strategies for cranial proton therapy: potential and challenges. *Radiat Oncol*. 2022;17(1):1-13. doi:10.1186/S13014-022-02143-X

28. Hahn C, Ödén J, Dasu A, et al. Towards harmonizing clinical linear energy transfer (LET) reporting in proton radiotherapy: a European multi-centric study. *Acta Oncol*. 2021(2):214. doi:10.1080/0284186X.2021.1992007

29. Källman P, Ågren A, Brahme A. Tumour and normal tissue responses to fractionated non-uniform dose delivery. *Int J Radiat Biol*. 1992;62(2):249-262. doi:10.1080/09553009214552071

30. Cronqvist AKarin Å. *Quantification of the response of heterogeneous tumours and organized normal tissues to fractionated radiotherapy*. Stockholm University; 1995.

31. Niemierko A, Schuemann J, Niyazi M, et al. Brain necrosis in adult patients after proton therapy: is there evidence for dependency on linear energy transfer? *Int J Radiat Oncol Biol Phys*. 2021;109(1):109-119. doi:10.1016/J.IJROBP.2020.08.058

32. Garbacz M, Cordoni FG, Durante M, et al. Study of relationship between dose, LET and the risk of brain necrosis after proton therapy for skull base tumors. *Radiother Oncol*. 2021;163:143-149. doi:10.1016/J.RADONC.2021.08.015

33. Giantsoudi D, Sethi RV, Yeap BY, et al. Incidence of CNS injury for a cohort of 111 patients treated with proton therapy for medulloblastoma: LET and RBE associations for areas of injury. *Int J Radiat Oncol Biol Phys*. 2016;95(1):287-296. doi:10.1016/J.IJROBP.2015.09.015

34. Ödén J, Toma-Dasu I, Witt Nyström P, Traneus E, Dasu A. Spatial correlation of linear energy transfer and relative biological effectiveness with suspected treatment-related toxicities following proton therapy for intracranial tumors. *Med Phys*. 2020;47(2):342-351. doi:10.1002/mp.13911

35. Bertolet A, Abolfath R, Carlson DJ, et al. Correlation of LET with MRI changes in brain and potential implications for normal tissue complication probability for patients with meningioma treated with pencil beam scanning proton therapy. *Int J Radiat Oncol Biol Phys*. 2022;112(1):237-246. doi:10.1016/J.IJROBP.2021.08.027

36. Grün R, Friedrich T, Traneus E, Scholz M. Is the dose-averaged LET a reliable predictor for the relative biological effectiveness? *Med Phys*. 2019;46(2):1064-1074. doi:10.1002/MP.13347

37. Magrin G, Palmans H, Stock M, Georg D. State-of-the-art and potential of experimental microdosimetry in ion-beam therapy. *Radiother Oncol*. 2023;182:109586. doi:10.1016/J.RADONC.2023.109586

38. Lühr A, von Neubeck C, Helmbrecht S, Baumann M, Enghardt W, Krause M. Modeling in vivo relative biological effectiveness in particle therapy for clinically relevant endpoints. *Acta Oncol*. 2017;56(11):1392-1398. doi:10.1080/0284186X.2017.1356468

39. DeCunha JM, Newpower M, Mohan R. GPU-accelerated calculation of proton microdosimetric spectra as a function of target size, proton energy, and bounding volume size. *Phys Med Biol*. 2023;68(16):160512. doi:10.1088/1361-6560/ACE60A

40. Tian L, Hahn C, Lühr A. An ion-independent phenomenological relative biological effectiveness (RBE) model for proton therapy. *Radiother Oncol*. 2022;174:69-76. doi:10.1016/J.RADONC.2022.06.023

41. Sánchez-Parcerisa D, López-Aguirre M, Dolcet Llerena, A, Udías JM. MultiRBE: treatment planning for protons with selective radiobiological effectiveness. *Med Phys*. 2019;46(9):4276-4284. doi:10.1002/MP.13718

42. Hahn C, Eulitz J, Peters N, et al. Impact of range uncertainty on clinical distributions of linear energy transfer and biological effectiveness in proton therapy. *Med Phys*. 2020;47(12):6151-6162. doi:10.1002/mp.14560

43. Grün R, Friedrich T, Krämer M, et al. Physical and biological factors determining the effective proton range. *Med Phys*. 2013;40(11). doi:10.1118/1.4824321

44. Traneus E, Jakob O. Introducing proton track-end objectives in intensity modulated proton therapy optimization to reduce linear energy transfer and relative biological effectiveness in critical structures. 2019;103(3):747-757. doi:10.1016/j.ijrobp.2018.10.031

45. Giantsoudi D, Grassberger C, Craft D, Niemierko A, Trofimov A, Paganetti H. Linear energy transfer-guided optimization in intensity modulated proton therapy: feasibility study and clinical potential. *Int J Radiat Oncol Biol Phys*. 2013;87(1):216-222. doi:10.1016/J.IJROBP.2013.05.013

46. Liu C, Patel SH, Shan J, et al. Robust optimization for intensity modulated proton therapy to redistribute high linear energy transfer from nearby critical organs to tumors in head and neck cancer. *Int J Radiat Oncol Biol Phys*. 2020;107(1):181-193. doi:10.1016/J.IJROBP.2020.01.013

47. Gu W, Ruan D, Zou W, Dong L, Sheng K. Linear energy transfer weighted beam orientation optimization for intensity-modulated proton therapy. *Med Phys*. 2021;48(1):57-70. doi:10.1002/MP.14329

48. Henjum H, Dahle TJ, Fjæra LF, et al. The organ sparing potential of different biological optimization strategies in proton therapy. *Adv Radiat Oncol*. 2021;6(6):100776. doi:10.1016/J.ADRO.2021.100776

49. Newpower M, Patel D, Bronk L, et al. Using the proton energy spectrum and microdosimetry to model proton relative biological effectiveness. *Int J Radiat Oncol Biol Phys*. 2019;104(2):316-324. doi:10.1016/J.IJROBP.2019.01.094

SUPPORTING INFORMATION

Additional supporting information can be found online in the Supporting Information section at the end of this article.